Original Article

Combinatorial Treatment of Mupirocin Nanomicelle in Insulin-Based Gel for Wound Healing in Diabetic Rats

Maysaa Banay Zubairi, Abdulkareem Hameed Abd[1], Mohammed Sabar Al-lami[2]

Department of Pharmacology and Toxicology, College of Pharmacy, University of Basrah, Basrah, [1]Department of Pharmacology, College of Medicine, Al-Nahrain University, Baghdad, [2]Department of Pharmaceutics, College of Pharmacy, University of Basrah, Basrah, Iraq

Abstract

Background: Diabetic wounds remain an important clinical challenge over the past few decades. Nanodrug delivery systems play a crucial role in the treatment of chronic infections and wound healing. **Objectives:** To evaluate the wound healing potential of newly synthesized and characterized mupirocin (MP) nanomicelle (NM) in insulin (I)-based gel (MP-NM-I), utilizing alloxan-induced diabetic rat model. **Materials and Methods:** MP-NM-I was prepared by solvent evaporation technique, 96 male rats were assigned randomly into eight groups (n = 12): one group is healthy, and the remaining seven groups were diabetic and wounded receiving treatments of gel base, tween 80, I, MP, MP-I, MP-NM, and MP-NM-I, respectively. Rats were sacrificed after 7 and 14 days of wounding. Blood samples were collected for glucose and insulin concentration measurement. Skin biopsies were examined by histological and immunohistochemical analyses. **Results:** Diabetes was confirmed after a significant increase in blood glucose and a decrease in serum insulin concentrations ($P \leq 0.001$). MP-NM– and MP-NM-I–treated groups presented a rapid wound closure (100 ± 0, $P \leq 0.001$), and the bacterial growth in these samples was relatively low ($P \leq 0.001$). Histological examination established a significant decrease in inflammatory cells ($P \leq 0.001$) with a significant elevation in tissue re-epithelialization, fibroblasts, angiogenesis, and collagen fibers ($P \leq 0.001$). Immunohistochemical investigation presented a significant decrease in tumor necrosis factor-α, increase in vascular endothelial growth factors, and interleukin-10 scores ($P \leq 0.001$). **Conclusion:** The developed formula of MP-NM with or without insulin is more effective than MP alone for diabetic wound healing in rats, because it accelerated wound closure. Accordingly, the formula might serve as an innovative tool for diabetic wound healing.

Keywords: Diabetic wound, insulin, mupirocin, nanomicelle

Introduction

Wound healing involves dynamic and complex processes including a number of intersecting phases such as hemostasis, inflammation, proliferation, and tissue remodeling, as illustrated in Figure 1.[1] Healing delay commonly presents in diabetic wounds as a result of improper re-epithelialization, vascular inefficiency, and chronic inflammation. Literature clarifies that diabetic wounds mediate about 50%–70% of entire leg amputations.[2,3]

Nanodrug delivery systems (Nano-DDSs) have been adopted for the treatment of wounds and chronic infections.[4] Nano-DDSs display a potential interaction in the enhancement of drug therapeutic efficacy by preventing drug degradation and sustaining drug release.[5] Different nano-DDSs carrying diagnostic and therapeutic agents are adopted in diabetic wound healing and cutaneous regeneration; mainly including liposomes, polymeric, lipid inorganic nanoparticles, micelles, and nanohydrogel.[6] Nanomicelle (NM) is comprised of a core and a shell, which exhibit hydrophobic and hydrophilic properties, respectively. It has a great capacity to inhibit the degradation of drugs, to diminish their side effects, and to improve drug permeation through tissues.[7]

Access this article online

Quick Response Code:

Website: https://journals.lww.com/mjby

DOI: 10.4103/MJBL.MJBL_189_23

Address for correspondence: Dr. Maysaa Banay Zubairi, Department of Pharmacology and Toxicology, College of Pharmacy, University of Basrah, Basrah, Iraq.
E-mail: phmaysaaalbasri@gmail.com

Submission: 21-Feb-2023 **Accepted:** 20-Apr-2023 **Published:** 02-Feb-2024

How to cite this article: Zubairi MB, Abd AH, Al-lami MS. Combinatorial treatment of mupirocin nanomicelle in insulin-based gel for wound healing in diabetic rats. Med J Babylon 2023;20:721-31.

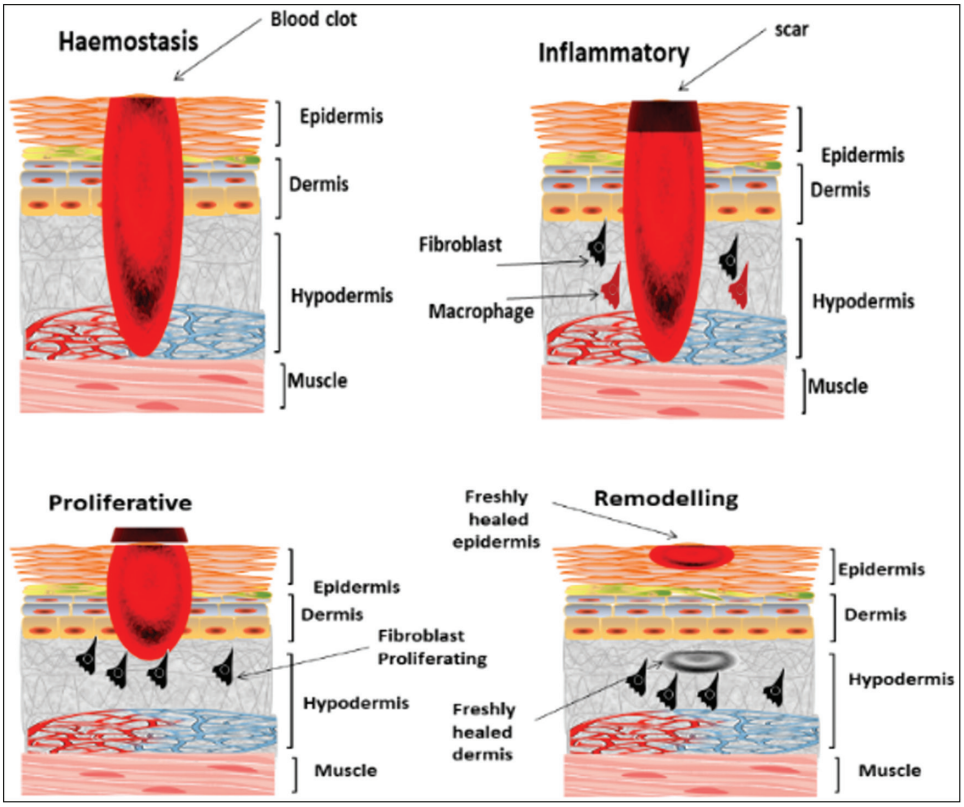

Figure 1: Phases of wound healing include: hemostasis, inflammation, proliferation, and remodeling phase

Mupirocin (MP) is a worldwide utilized topical antibiotic for the treatment of a variety of bacterial cutaneous infections because of its unique mechanism involving inhibition of protein and RNA synthesis, by binding to and blocking the formation of bacterial isoleucyl-tRNA synthetase in *Staphylococcus aureus, Streptococcus pyogenes*, and *Escherichia coli*.[8] However, the therapeutic effectiveness is impeded due to resistance, high protein binding, and relatively short half-life. MP efficacy can be potentiated by formulating a biocompatible nanocarrier that supports and promotes proliferation and cell growth.[9]

The aim of our study was to examine the newly synthesized and characterized formula of MP-NM-I in terms of the wound healing potential by evaluating histological and biochemical parameters; and to assess the mechanism of wound healing in laboratory animals, utilizing alloxan-induced diabetic rat model.

Materials and Methods

Materials

MP pure powder and Tween 80 were obtained from Baoji Guokang Bio-Technology Co., Ltd (City Mansion, China). Hydroxypropyl methylcellulose (HPMC) polymer, grade E10M, was obtained from Wallocell (Randstad, Netherlands). Ketamine hydrochloride 100 mg/mL and Xylazine hydrochloride 20 mg/mL were bought from Bayer (Leverkusen, Germany). Soluble Insulin was supplied by Eli Lilly and Co. (Indanapolis, Indiana). Antitumor necrosis factor (TNF-α) antibody ab2202 and DAB detection kit were provided by Abcam (Cambridge, UK). Interleukin-10 (IL-10) polyclonal antibody and vascular endothelial growth factors (VEGFs) monoclonal antibody were provided by Thermofisher, Waltham, MA, USA. Insulin ELISA kit was obtained from ALPCO, Salem, United States.

Methods

Preparation and characterization of mupirocin-loaded nanomicelle in insulin-based gel

A solvent evaporation technique was employed for the preparation of MP-NM in a 4% ratio[10]; by the addition of 200 mg MP to 0.9 mL Tween 80 in 5-mL ethanol. After evaporation at a temperature of 40–45°C, deionized water was added. For gel synthesis, HPMC polymer was dissolved in boiling water, then 0.1 mL soluble insulin was added to 4.84 mL of gel and 5.06 mL of MP-NM to prepare the final formulation MP-NM-I.

Photon correlation spectroscopy (Zetasizer NanoZS, Malvern Instrument, Malvern, Worcestershire, UK) was used to quantify the mean spherical diameter and polydispersity index (PDI) of the MP-NM. Furthermore, dialysis membrane (3.5 Kd cutoff) was utilized as closed-ended tape for the measurement of entrapment efficiency (EE). A total of 1 mL MP-NM, comprising 40 mg MP, was placed on the membrane; this underwent centrifugation (6000 rpm) to segregate the free nontrapped MP from the remaining preparation.[11]

In vitro irritation study

To study the potential of irritation, hen's egg-chorioallantoic membrane (CAM) test was performed. Eggs were incubated at 37.5 ± 0.5°C and a humidity of 40% ± 4%. On day 10 of incubation, the shell was cracked and removed. A total of 0.2 mL MP-NM-I was dropped onto the yolk. Sodium hydroxide (NaOH) (0.1 M) and normal saline (0.2 mL each) were used as positive and negative controls, respectively. Irritancy was calculated in terms of irritation score.[12,13]

Experimental animals

Ninety-six adult male rats (8–12 weeks of age; and body weight 200–300 g) were used. All experimental procedures were approved by local Ethics Committee of Institute Review Board (no: 202010104 on January 10, 2021). Rats were assigned randomly into eight experimental groups, each containing 12 rats, six of them were sacrificed after 7 days of wounding, and the remaining six were sacrificed after 14 days.[14,15] Groups of animals are listed as follows (treatments were applied twice daily on wounds):

Group H: Apparently healthy (nondiabetic, unwounded, and untreated)

Group G: Diabetic wounded treated with gel only

Group I: Diabetic wounded treated with gel + insulin

Group MP: Diabetic wounded treated with gel + MP

Group MP-I: Diabetic wounded treated with gel + insulin + MP

Group MP-NM: Diabetic wounded treated with gel + MP-NM

Group MP-NM-I: Diabetic wounded treated with gel MP-NM-I

Alloxan-induced diabetic model

Rats received a single intraperitoneal (I.P.) injection of alloxan solution (90 mg/kg). On the seventh day after alloxan injection, blood glucose measurement was performed, and rats whose fasting blood glucose exceeded 250 mg/dL were considered diabetic.[16]

Blood glucose and serum insulin concentrations

Blood glucose levels were determined using glucometer (Accu-Chek, Taguig, Philippines). Insulin ELISA kit was designed for the quantitative estimation of serum insulin by sandwich immunoassay. The 96-well microplate was coated with insulin-specific monoclonal antibodies. The controls, standards, and samples were added to the detection antibody and then incubated on a microplate shaker at 700 rpm. The colored product was measured.

White blood cells and body weight measurement

White blood cells (WBCs) were counted at arrival and the end of the study after collecting blood from the rats in etheylenediaminetetraacetic acid-containing tube, quantified using complete blood count apparatus (Guangzhou, China). Body weight was recorded at arrival, and at the end of the study using an electronic balance.

Surgical wound model and specimen collection

After 2 months of alloxan-induced diabetes mellitus, diabetic rats were generally anesthetized by I.P. administration of ketamine and xylazine. Dorsal surface was shaved and decontaminated. A punch biopsy instrument was used to create a full thickness-round wound (diameter, 8 mm) in the upper back of rat. The prepared treatments were applied on the wounds.[17] Wound diameter in mm was measured for each rat at day 0 (promptly after wounding), 3, 5, 7, 10, 12, and 14 postoperations. The percentage (%) of wound contraction was measured.[18]

Wound contraction %= (The original wound area − The wound area at the imaging time)/The original wound area × 100.

On days 7 and 14 postoperation, tissue biopsies of wounds were taken, and biopsies were fixed in 10% formalin solution. Formalin-fixed paraffin-embedded block was cut into 5-µm slices and stained with hematoxylins to examine the histopathological and immunohistochemical (IHC) properties. The scale was evaluated semiquantitatively as: absent, 0; mild, 1; moderate, 2; and marked, 3.[19,20]

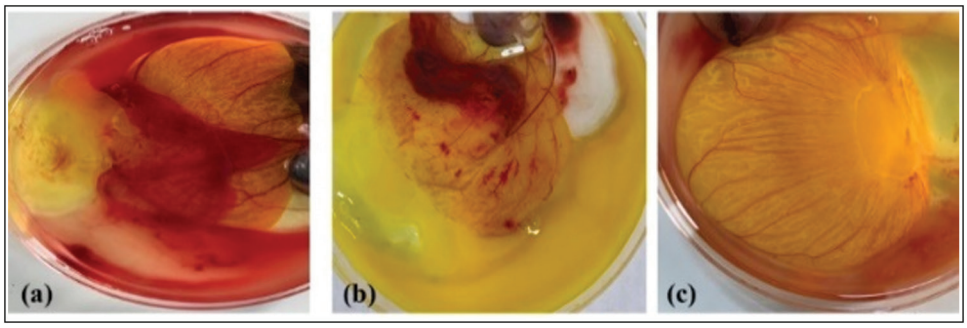

Figure 2: Vascular reactions to the CAM surface after application: (a) normal saline, (b) NaOH 0.1 M, and (c) MP-NM-I. MP-NM-I: mupirocin nanomicelle in insulin-based gel

In vitro antibacterial assay

Media was prepared by dissolving agar powder in 500 mL of water. Subsequently, the agar was sterilized by autoclave (25°C for 45 min) before pouring it into Petri dishes. On day 7 after wounding, just before sacrificing, swapping the wound was achieved by gently rotating a sterile cotton swab with enough pressure. Swaps were dipped in 5-mL normal saline to count colony-forming units (CFUs).[21]

$$\text{CFUs/mL of sample} = \text{Number of colonies} \times \text{Dilution factor}$$

Statistical analysis

Microsoft Office Excel 2021 , Impressa Systems, Santa and GraphPad Prism 8 software packages (GraphPad Software, Boston, USA) were utilized for data analysis and presentation. Numerical variables were expressed as mean ± standard deviation; Student's two-tailed paired *t* test was applied unless noted otherwise. A *P*-value of less than 0.05 was deemed to be significant, and a *P*-value of more than 0.05 was declared to be insignificant.[22]

Table 1: Cumulative scores of irritation potential calculation

Substances	Irritation potential (numerical score)	
	Practically non (0–0.9)	Strong (9–21)
Normal saline	√	
NaOH (0.1 M)		√
MP-NM-I	√	

MP-NM-I: mupirocin nanomicelle in insulin-based gel, NaOH, sodium hydroxide

Results

Preparation and characterization of mupirocin nanomicelle in insulin-based gel

The preparation of MP-NM generated in this study was completely clear; the MP was totally dissolved with no visible precipitation of the drug. The formulations were noted to have an expected homogeneous dispersion and globular size (PDI, 0.143 ± 0.003; and globular diameter, 8.648 ± 0.2 nm). The free drug present and EE value obtained were 1.15% ± 0.01% and 98.85% ± 0.01%, respectively.

Irritation study

Normal saline revealed no effect on the surface of the CAM. On the contrary, NaOH produced a remarkable irritation response with blood vessel hemorrhage, lysis, coagulation, and hyperemia. MP-NM-I was shown to be basically nonirritant [Figure 2 and Table 1].

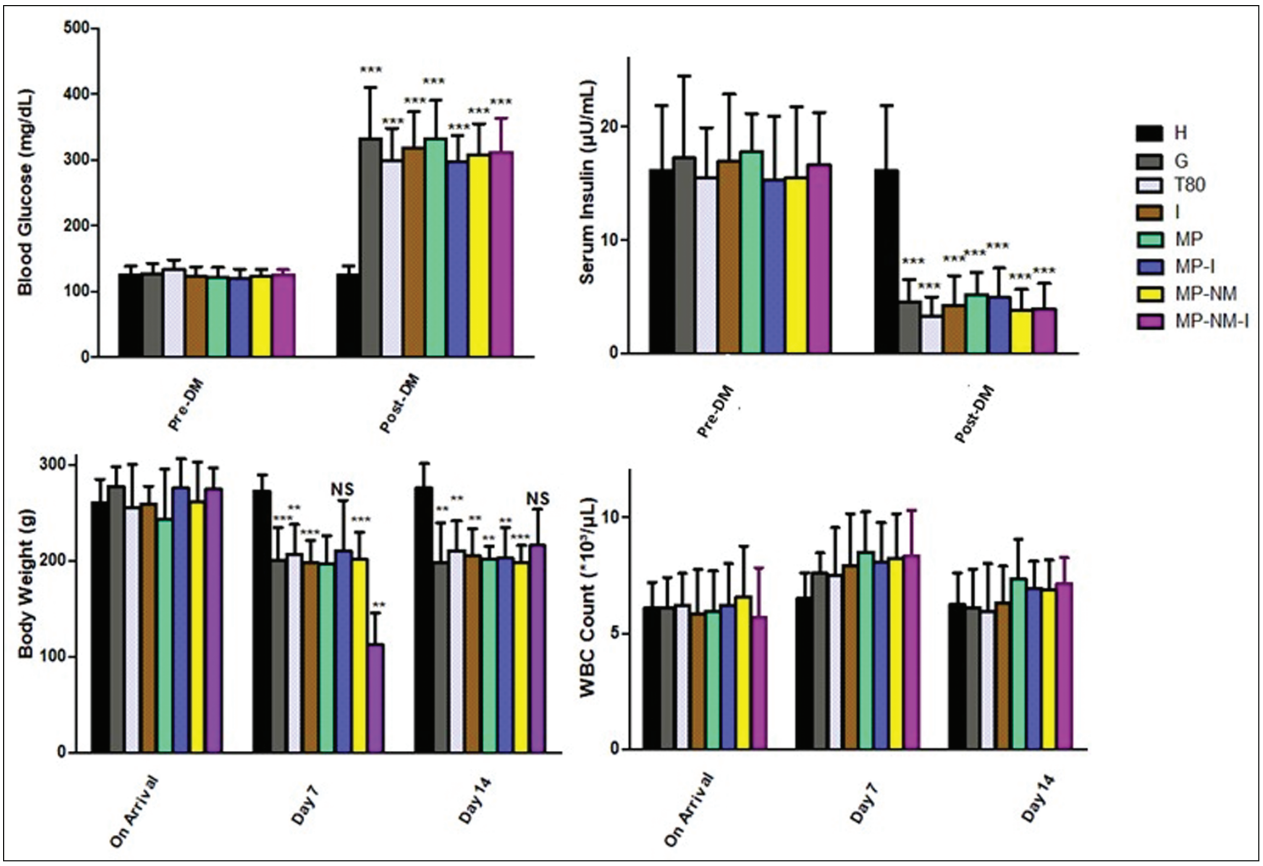

Figure 3: Effect of diabetes induction on physical and biochemical parameters. ***$P \leq 0.001$, **$P \leq 0.01$, *$P \leq 0.05$; significant changes compared with healthy group. NS: nonsignificant

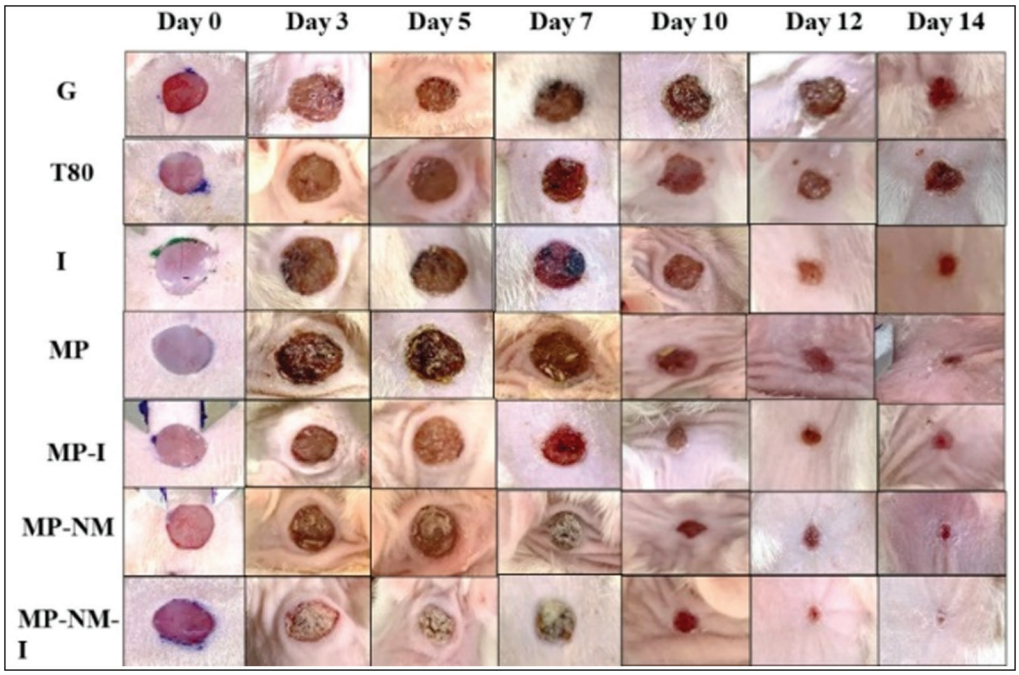

Figure 4: Serial photographs of wounds in diabetic rats' treatment groups on different days

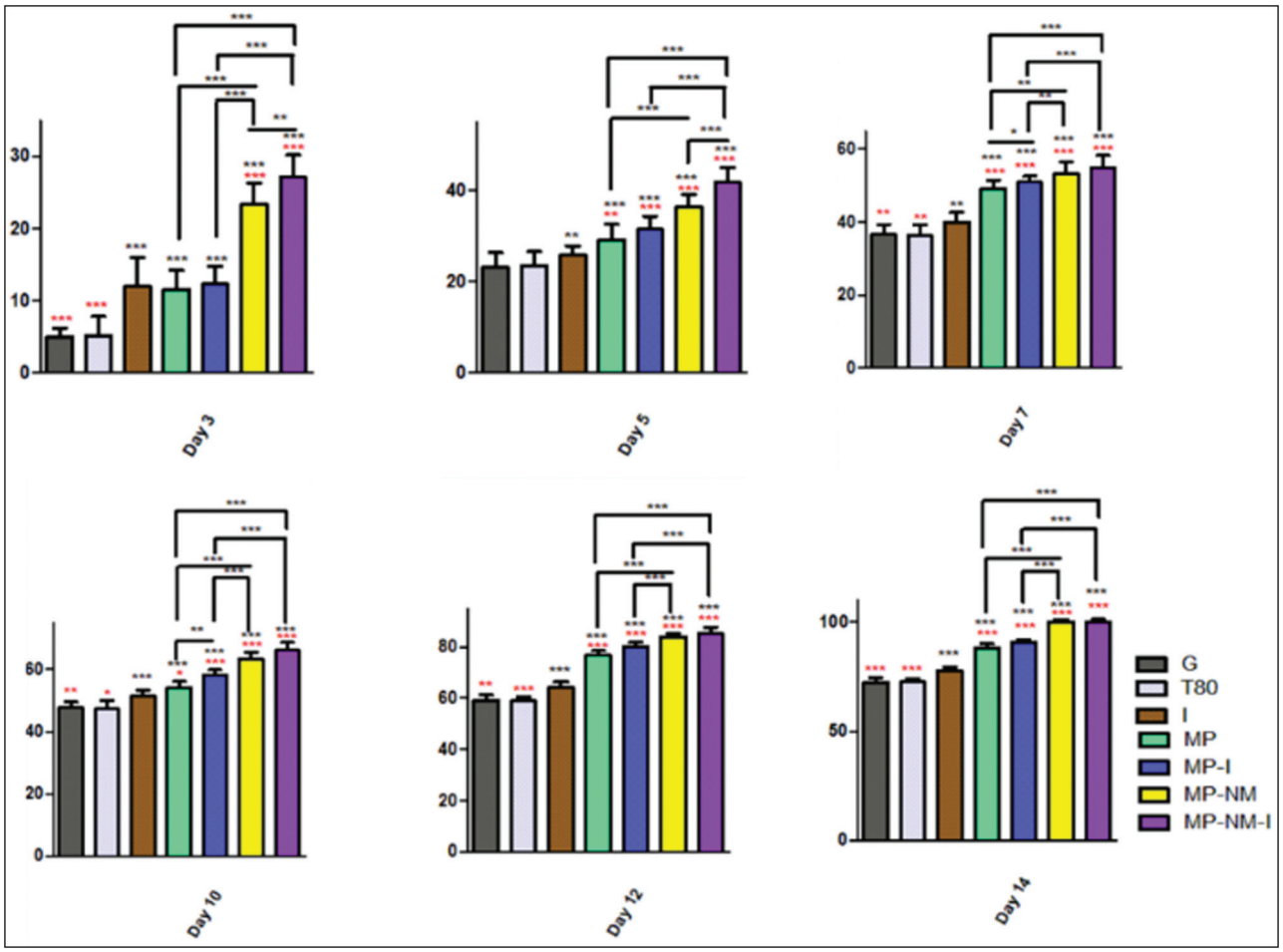

Figure 5: Effect of various treatments on wound contraction area percentage on postwounding days ***$P \leq 0.001$, **$P \leq 0.01$, *$P \leq 0.05$; significant changes compared with gel-treated group. Red stars: significant changes compared with insulin-treated group

Blood parameters and body weight findings

The results displayed a highly significant increase in blood glucose and a decrease in serum insulin concentrations in diabetic groups ($P \leq 0.001$). Also, it demonstrated a significant reduction in body weight in diabetic rats compared with the nondiabetics ($P \leq 0.001$) ($P \leq 0.01$). No significant differences were found in WBCs count between diabetic and nondiabetic rats throughout the study ($P < 0.05$) [Figure 3].

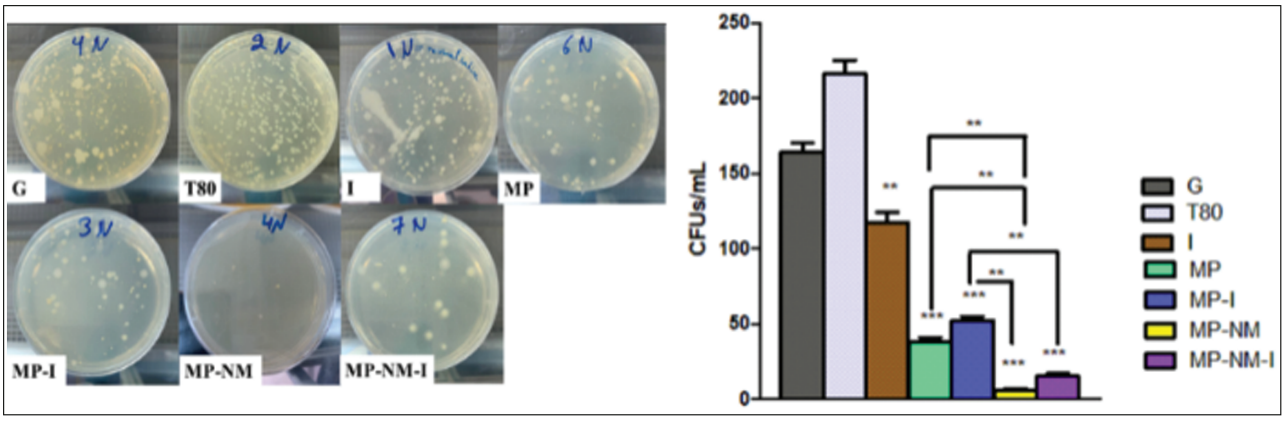

Figure 6: Colony-forming units per milliliter of cultured samples. ***$P \leq 0.001$, **$P \leq 0.01$; significant difference from gel-treated group

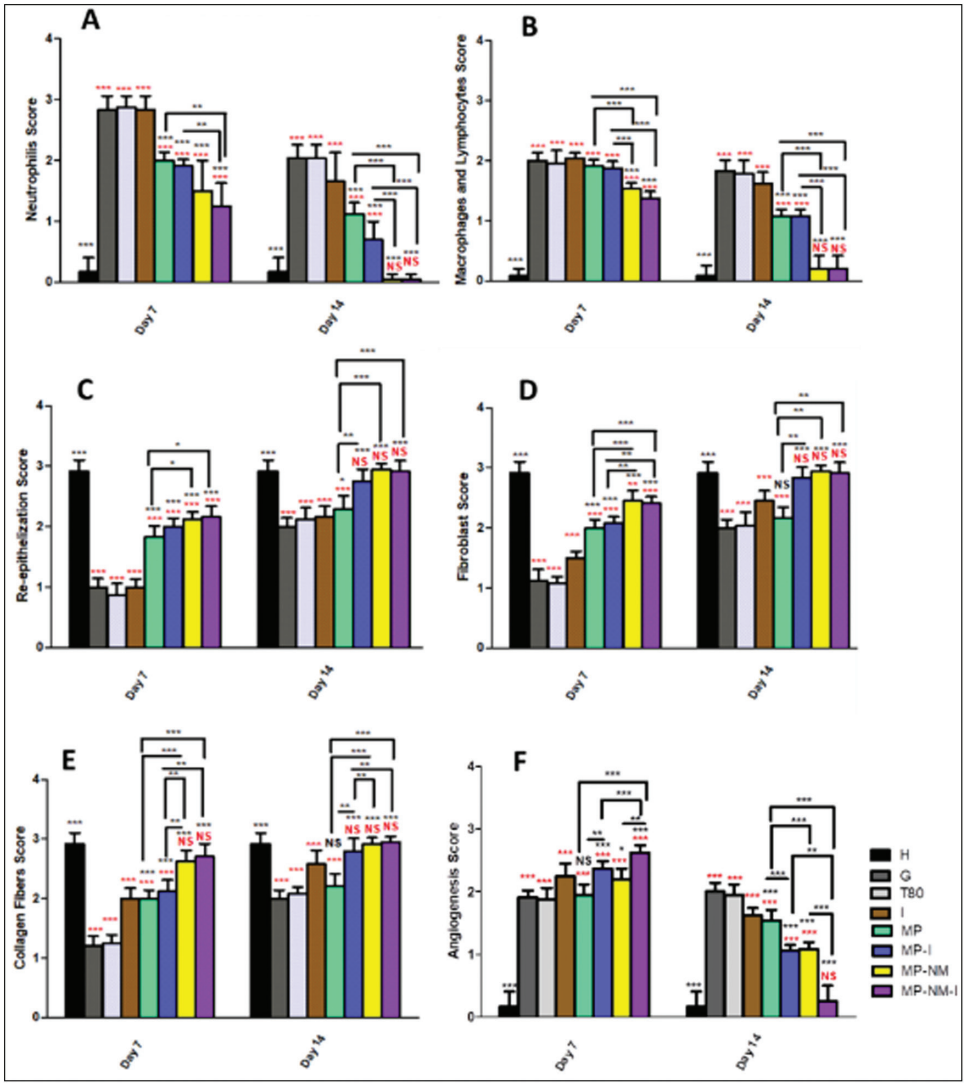

Figure 7: Effect of various treatments on histological parameters on postwounding day 7 and 14. ***$P \leq 0.001$, **$P \leq 0.01$, *$P \leq 0.05$; significant difference compared with gel-treated group. NS: nonsignificant ($P > 0.05$). Red stars: significant difference compared with healthy group

Morphological wound healing

Wound contraction area percentage was measured in all examined groups, as shown in Figures 4 and 5. It was detected that all the treated groups displayed significantly better findings in terms of wound healing. Significant differences in the wound closure rate were shown in groups treated with MP-NM and MP-NM-I compared with other treated animals (day 7, 53.1 ± 3.31 and 54.7 ± 2.24, respectively, whereas both on day 14, 100 ± 0) ($P \leq 0.001$). Importantly, the novel formula MP-NM-I promoted significant wound closure compared with MP- and MP-I–treated rats ($P \leq 0.001$).

Wound colonization

The cultures showed uneven growth of bacteria (*S. aureus* or anaerobic organisms) for different treatment groups. The bacterial growth in dishes cultured with I, MP, MP-I, MP-NM, and MP-NM-I treated groups ($117 \pm 7 \times 10^5$, $38 \pm 3 \times 10^5$, $52 \pm 3 \times 10^5$, $6 \pm 1 \times 10^5$, $15 \pm 2 \times 10^5$, respectively) presented a significant decrease in CFUs/mL compared with gel-treated group ($164 \pm 6 \times 10^5$) ($P \leq 0.001$) [Figure 6]. Essentially, there was a significant decrease in CFUs/mL of MP-NM– and MP-NM-I–treated groups compared with MP- and MP-I–treated groups ($P \leq 0.01$).

Histopathological and immunohistochemical findings

Neutrophiles, macrophages, and lymphocytes score on day 7 postwounding showed a significant rise in all treated groups compared with apparently healthy group ($P \leq 0.001$). On the same day, MP, MP-I, MP-NM, and MP-NM-I treated groups showed significant decrease in these parameters in comparison with gel-treated group ($P \leq 0.001$). Our novel formulas, MP-NM and MP-NM-I (neutrophiles, 0.04 ± 0.09; macrophages and lymphocytes, 0.2 ± 0.22 for both groups), showed no significant differences in comparison with apparently healthy group on day 14 (neutrophiles, 0.04 ± 0.09; macrophages and lymphocytes, 0.08 ± 0.11) ($P < 0.05$). Skin tissue re-epithelialization, fibroblasts, collagen fibers, and angiogenesis level on day 7 have a significant decrease in all treated groups compared with apparently healthy rats ($P \leq 0.001$). MP, MP-I, MP-NM, and MP-NM-I treated groups significantly increased in these parameter scores in comparison with gel-treated group ($P \leq 0.001$). Interestingly, the novel formulas, MP-NM and MP-NM-I (re-epithelialization, 2.95 ± 0.09 and 2.91 ± 0.18; fibroblasts, 2.95 ± 0.09 and 2.91 ± 0.18; collagen, 2.91 ± 0.11 and 2.95 ± 0.09; and angiogenesis, 1.08 ± 0.11 and 0.25 ± 0.25, respectively), showed no significant differences in comparison with apparently healthy group on day 14 (re-epithelialization, 2.95 ± 0.09; fibroblasts, 2.95 ± 0.09; collagen, 2.91 ± 0.18; and angiogenesis, 0.16 ± 0.23) ($P < 0.05$) [Figures 7 and 8].

As illustrated in Figures 9 and 10, TNF-α score on day 7 showed a significant increase in all treated groups compared with healthy group ($P \leq 0.001$). On days 7 and 14, MP, MP-I, MP-NM, and MP-NM-I treated groups significantly decreased in comparison with gel-treated animals ($P \leq 0.001$). MP-NM and MP-NM-I presented no significant differences in comparison with apparently healthy on day 14 (0.08 ± 0.11 of both groups vs. 0.08 ± 0.11 of healthy) ($P < 0.05$). VEGF and IL-10 activity on day 7 presented a significant increase in all treated animals compared with healthy group ($P \leq 0.001$). On day 14, the later parameters decreased compared with gel group when treated with MP, MP-I, MP-NM, and MP-NM-I

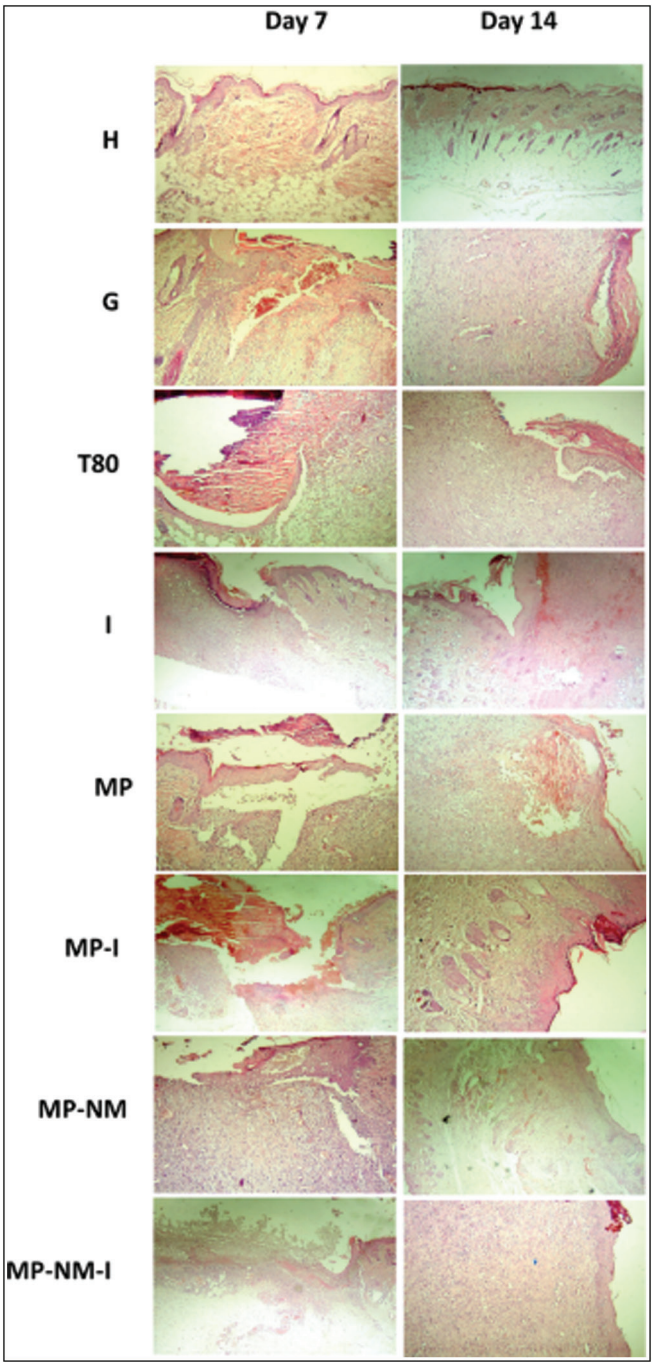

Figure 8: Histopathological changes in skin tissues on day 7 and 14 posttreatments. Hematoxylin and Eosin stain (4× and 10×)

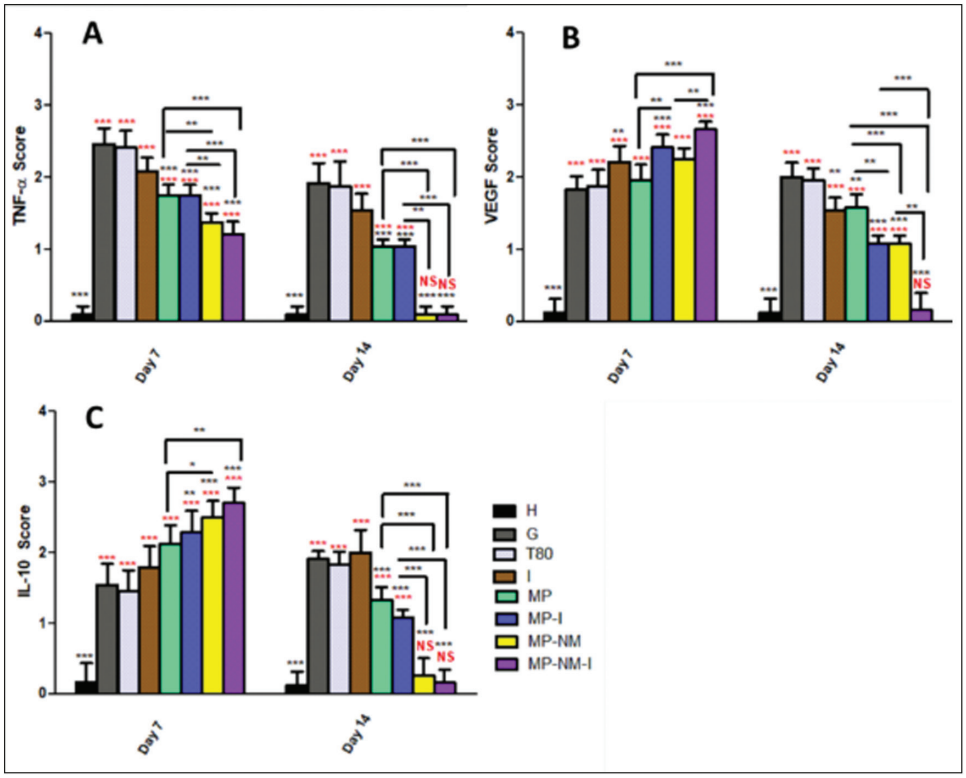

Figure 9: Effect of various treatments on immunohistochemical parameters. ***$P \leq 0.001$, **$P \leq 0.01$, *$P \leq 0.05$; significant difference compared with gel-treated group. NS: nonsignificant ($P > 0.05$). Red stars: significant difference compared with healthy group

($P \leq 0.001$). No significant difference was detected when an animal treated with MP-NM and MP-NM-I (VEGF, 1.08 ± 0.11 and 0.16 ± 0.23; and IL-10, 0.25 ± 0.25 and 0.16 ± 0.18, respectively) in comparison with healthy group on day 14 (VEGF, 0.12 ± 0.19; and IL-10, 0.12 ± 0.19) ($P < 0.05$).

Discussion

Management of wound infections using traditional antibacterial strategies becomes a critical condition, there is an urgent need to develop novel approaches for this purpose. Nanotechnology has appeared as an efficient approach in this field.[23]

In our lab, MP is dissolved by NM through its entrapment within the mixed micellar hydrophobic core; the clear aqueous solution is facilitated by a corona of hydrophilic chains.[24] A relatively high volume of Tween 80 was utilized to achieve the current nanosized particle. Tween 80 showed an excellent behavior; it promotes the generation of smaller drug particles.[25] A proper selection of the type and concentration of surfactant used has been shown to demonstrate a significant impact on the entrapping efficiency of the synthesized NM.[26] This implies that the NM has a compact structure and a potent interaction between surfactant and drug.

Many studies demonstrated that MP has a favorable effect on the rate of wound contraction, period of epithelization, and collagen content of wound in diabetic rats.[27] However, this was mainly due to its antibacterial role; also, it may promote wound closure through the enhancement of keratinocytes proliferation.[28] All these are consistent with our results.

Treatment with MP-NM produced rapid wound healing by forming a distinctive white rough layer on the wound that was not seen in all other groups [Figure 11]. This layer appeared around day 7 and converted to complete fibrosis on day 14. Porosity and stability of the formula were the key causes for the amplified adsorption of the water occurs that in wound exudate, forming this layer on the wound surface and the boost of autolytic debridement of the wound infection.[29]

MP-NM-I possessed better antimicrobial effectiveness and could be safely administered to the infected area. The formula boosts the antimicrobial effect against various pathogens present in wound probably through the enhanced retention of MP in the skin.[30]

Assessment of histopathological changes is an integral step to approve the role of MP-NM-I–mediated wound healing. The accelerated wound-healing efficacy of MP-NM-I is probably due to modulating the inflammatory phase. MP-NM-I–treated group demonstrated a dramatic improvement in collagen synthesis, re-epithelialization, and fibrosis, as well as ameliorated the level of TNF-α and supported rate-limiting steps of angiogenesis.

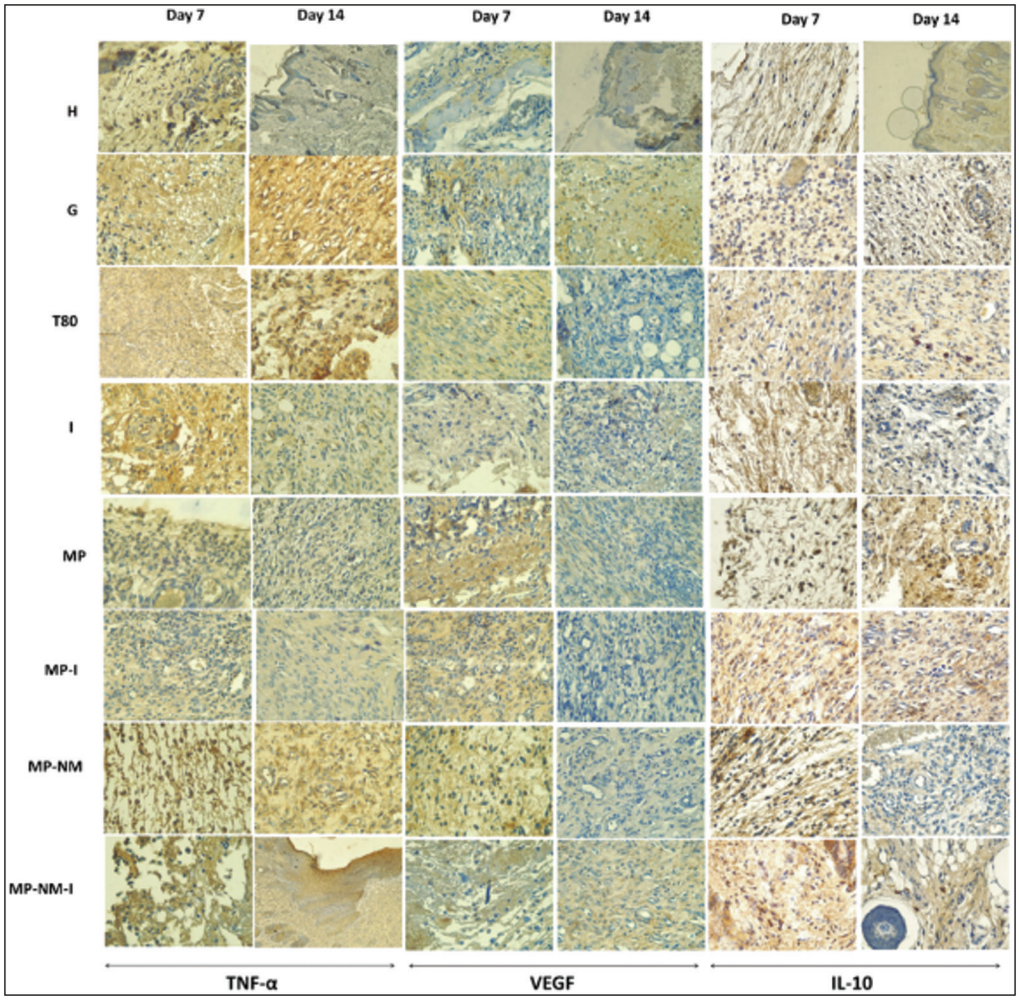

Figure 10: Immunohistochemical changes in skin tissues on day 7 and 14 posttreatment (4×, 10×, and 40×)

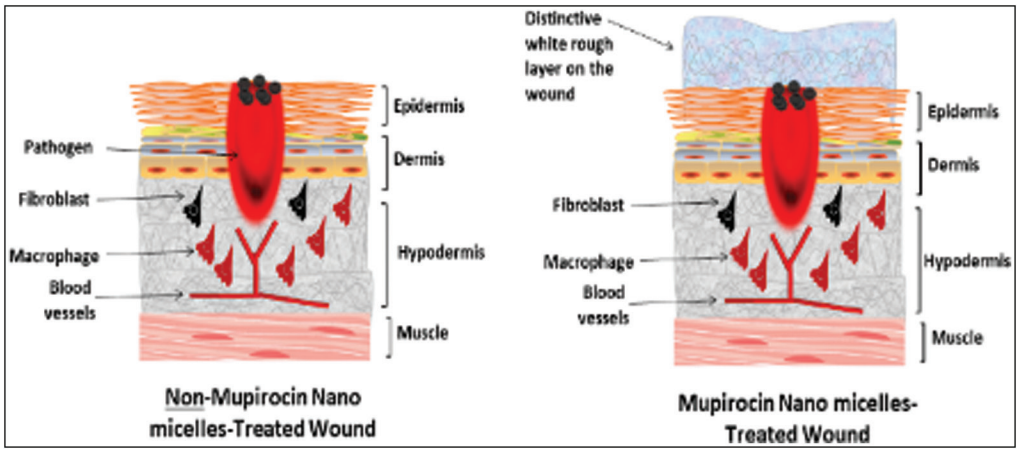

Figure 11: Mupirocin nanomicelle treated wound showing a distinctive layer of fibrous meshwork

MP-NM– and MP-NM-I–treated groups showed a mature denes collagen fiber. This result is consistent with other studies, which stated that wound healing in diabetic mice after nanoparticles shows an increase in collagen deposition, stimulation of fibroblast activity, and acceleration of wound repair.[31,32] Various studies on wound healing including diabetic animals approved that many drugs loaded with nanoparticles improved re-epithelialization, angiogenesis, and VEGF-A.[33] The nanosized particles play a crucial role in the absorption and pharmacokinetic properties of locally applied nanocarriers. After the administration into the wound bed

and penetration into the subcutaneous tissue, nanomicelle carriers smaller than 10 nm may reach the lower strata of the dermis and may be absorbed by the blood capillaries.[34]

MP alone significantly decreases inflammatory cell infiltration. Only a few studies have reported this effect.[35] The addition of insulin to MP-NM exhibited distinctive results that were consistent with many studies. Insulin plays a pivotal role in the regulation of glucose uptake by skin cells that stimulates keratinocytes migration and fibroblast proliferation.[36] Literature has presented that insulin modifies skin wound closure in diabetic clinical and subclinical studies.[37] Besides, the use of topical insulin in wounded skin increased the tissue expression of VEGF[38] and regulates IL-10 levels to eliminate dead tissues.[39]

MP-NM treatment ameliorated the level of TNF-α, and this result agrees with many previous studies about the nano-DDSs on IHC biomarkers in excisional wound healing. For example, topical treatment of different nanoparticle-loaded drugs decreased the levels of pro-inflammatory cytokine TNF-α, increased the levels of anti-inflammatory cytokine IL-10, and completed skin restoration.[40,41] Otherwise, IL-10 overexpression in MP-NM and MP-NM-I successfully decreases the inflammatory response to injury. There were fewer inflammatory cells recruited to the wound during the inflammatory phase, and this agrees with histological results.[42] Khezri *et al*.[43] reported that the treated animals' wounds with MP showed a higher concentration of IL-10 and VEGF. But the effect of nanoparticle-loaded drugs overcomes the effect of the native MP,[43] and this agrees with our findings. However, the completely healed wound of MP-NM and MP-NM-I had a negative score, but VEGF still appeared in other treated groups with relatively delayed healing.

Conclusions

It can be concluded that the novel formulas MP-NM and MP-NM-I promoted better wound healing compared with MP and MP-I in the diabetic rat. Although MP-NM demonstrated a significant antibacterial activity, it showed no irritation during the safety test. MP-NM-I–mediated wound healing can be attributed to dramatic improvement in inflammatory response, re-epithelialization, and fibrosis.

Financial support and sponsorship

Nil.

Conflict of interest

There are no conflicts of interest.

References

1. Syahputra IR. Wound healing response to full-thickness skin defect sprague dawley rats given ozonated black cumin oil viewing from the profile of neutrophil and macrophage count. Diponegoro Int Med J 2022;3:19-28.
2. Okur ME, Karantas ID, Siafaka PI. Diabetes mellitus: A review on pathophysiology, current status of oral medications and future perspectives. Acta Pharm Sci 2017;55:61-82.
3. Baiee HA, Makai MB. Medication adherence in hypertensive diabetic patients. Med J Babylon 2022;19:569.
4. Almuthaffer AM. Awareness and attitude on use of nanotechnology among dental and medical professionals in Iraq. Med J Babylon 2022;19:528.
5. Korrapati PS, Karthikeyan K, Satish A, Krishnaswamy VR, Venugopal JR, Ramakrishna S. Recent advancements in nanotechnological strategies in selection, design and delivery of biomolecules for skin regeneration. Mater Sci Eng C 2016;67:747-65.
6. Wang W, K-j L, C-h Y, Huang Q-l, Du Y-Z. Nano-drug delivery systems in wound treatment and skin regeneration. J Nanobiotechnol 2019;17:1-15.
7. Rehan F, Ahemad N, Gupta M. Casein nanomicelle as an emerging biomaterial—A comprehensive review. Colloids Surf B Biointerfaces 2019;179:280-92.
8. Khoshnood S, Heidary M, Asadi A, Soleimani S, Motahar M, Savari M, *et al*. A review on mechanism of action, resistance, synergism, and clinical implications of mupirocin against Staphylococcus aureus. Biomed Pharmacother 2019;109:1809-18.
9. Golmohammadi R, Najar-Peerayeh S, Tohidi Moghadam T, Hosseini SMJ. Synergistic antibacterial activity and wound healing properties of selenium-chitosan-mupirocin nanohybrid system: An in vivo study on rat diabetic staphylococcus aureus wound infection model. Sci Rep 2020;10:1-10.
10. Al Radhi MS, Al-Lami MS, Abdulsahib E. Preparation and characterization of diazepam loaded nanomicelles for pediatric intravenous dose adjustment. Int J Pharm Res 2021;13:2275-86.
11. Sharma D, Bhargava S, Kumar BJDD, Pharmacy I. Formulation and optimization for DPP-4 inhibitor nanomicelles using response surface methodology. Drug Dev Ind Pharm 2020;46:70-9.
12. Luepke N. Hen's egg chorioallantoic membrane test for irritation potential. Food Chem Toxicol 1985;23:287-91.
13. Smail SS, Ghareeb MM, Omer HK, Al-Kinani AA, Alany RG. Studies on surfactants, cosurfactants, and oils for prospective use in formulation of ketorolac tromethamine ophthalmic nanoemulsions. Pharmaceutics 2021;13:467.
14. Cheng K-Y, Lin Z-H, Cheng Y-P, Chiu H-Y, Yeh N-L, Wu T-K, *et al*. Wound healing in streptozotocin-induced diabetic rats using atmospheric-pressure argon plasma jet. Sci Rep 2018;8:1-15.
15. Mendes JJ, Leandro CI, Bonaparte DP, Pinto AL. A rat model of diabetic wound infection for the evaluation of topical antimicrobial therapies. Comp Med 2012;62:37-48.
16. Ighodaro OM, Adeosun AM, Asejeje FO, Soetan GO, Kassim OO. Time course effects of 5, 5-dihydroxyl pyrimidine-2, 4, 6-trione (alloxan) as a diabetogenic agent in animal model. Alexandria J Med 2018;54:705-10.
17. DiPietro LA, Burns AL. Wound Healing: Methods and Protocols. Springer; Maywood, USA: Loyola University Medical Center. 2003.
18. Yates CC, Whaley D, Babu R, Zhang J, Krishna P, Beckman E, *et al*. The effect of multifunctional polymer-based gels on wound healing in full thickness bacteria-contaminated mouse skin wound models. Biomaterials 2007;28:3977-86.
19. Gal P, Kilik R, Mokry M, Vidinsky B, Vasilenko T, Mozes S, *et al*. Simple method of open skin wound healing model in corticosteroid-treated and diabetic rats: Standardization of semi-quantitative and quantitative histological assessments. Vet Med 2008;53:652-9.
20. Kokolakis G, Panagis L, Stathopoulos E, Giannikaki E, Tosca A, Krüger-Krasagakis S. From the protein to the graph: How to quantify immunohistochemistry staining of the skin using digital imaging. J Immunol Methods 2008;331:140-6.
21. Rondas AA, Schols JM, Halfens RJ, Stobberingh EE. Swab versus biopsy for the diagnosis of chronic infected wounds. Adv Skin Wound Care 2013;26:211-9.
22. Ali Z, Bhaskar SB. Basic statistical tools in research and data analysis. Indian J Anaesth 2016;60:662.

23. Zare H, Rezayi M, Aryan E, Meshkat Z, Hatamluyi B, Neshani A, *et al*. Nanotechnology-driven advances in the treatment of diabetic wounds. Biotechnol Appl Biochem 2021;68:1281-306.
24. Velagaleti P, Anglade E, Khan I, Gilger B, Mitra A. Topical delivery of hydrophobic drugs using a novel mixed nanomicellar technology to treat diseases of the anterior and posterior segments of the eye. Drug Deliv Technol 2010;10:42-7.
25. Sukmawati A, Utami W, Yuliani R, Da'i M, Nafarin A, editors. Effect of Tween 80 on Nanoparticle Preparation of Modified Chitosan for Targeted Delivery of Combination Doxorubicin and Curcumin Analogue. IOP Conference Series: Materials Science and Engineering. Vol. 311, 2017 International Conference on Sensors, Materials and Manufacturing (ICSMM 2017) 24–26 November 2017. Chiayi, Taiwan: IOP Publishing; 2018.
26. Abdelbary G, Fahmy RH. Diazepam-loaded solid lipid nanoparticles: Design and characterization. AAPS Pharm Sci Tech 2009;10:211-9.
27. Bairy K, Nayak V, Kumar S, Adiga S, Holla A, Kumar P, *et al*. Comparative effect of sodium fusidate, framycetin and calcium mupirocin on experimentally induced burn wound healing. Int J Pharm Sci Bio 2010;1:100-2.
28. Twilley D, Reva O, Meyer D, Lall NJFP. Mupirocin promotes wound healing by stimulating growth factor production and proliferation of human keratinocytes. Front Pharmacol 2022;13:862112.
29. Zahedi P, Rezaeian I, Ranaei-Siadat SO, Jafari SH, Supaphol P. A review on wound dressings with an emphasis on electrospun nanofibrous polymeric bandages. Polym Adv Technol 2010;21:77-95.
30. Goldmann O, Cern A, Müsken M, Rohde M, Weiss W, Barenholz Y, *et al*. Liposomal mupirocin holds promise for systemic treatment of invasive Staphylococcus aureus infections. J Control Release 2019;316:292-301.
31. Blecher K, Martinez LR, Tuckman-Vernon C, Nacharaju P, Schairer D, Chouake J, *et al*. Nitric oxide-releasing nanoparticles accelerate wound healing in NOD-SCID mice. Nanomedicine 2012;8:1364-71.
32. Guthrie KM, Agarwal A, Teixeira LB, Dubielzig RR, Abbott NL, Murphy CJ, *et al*. Integration of silver nanoparticle-impregnated polyelectrolyte multilayers into murine-splinted cutaneous wound beds. J Burn Care Res 2013;34:e359-e67.
33. Chereddy KK, Her C-H, Comune M, Moia C, Lopes A, Porporato PE, *et al*. PLGA nanoparticles loaded with host defense peptide LL37 promote wound healing. J Control Release 2014;194:138-47.
34. Rigo C, Ferroni L, Tocco I, Roman M, Munivrana I, Gardin C, *et al*. Active silver nanoparticles for wound healing. Int J Mol Sci 2013;14:4817-40.
35. Kamlungmak S, Nakpheng T, Kaewpaiboon S, Bintang MAKM, Prom-In S, Chunhachaichana C, *et al*. Safety and biocompatibility of mupirocin nanoparticle-loaded hydrogel on burn wound in rat model. Biol Pharm Bull 2021;44:1707-16.
36. Emanuelli T, Burgeiro A, Carvalho E. Effects of insulin on the skin: Possible healing benefits for diabetic foot ulcers. Arch Dermatol Res 2016;308:677-94.
37. Liu Y, Petreaca M, Yao M, Martins-Green M. Cell and molecular mechanisms of keratinocyte function stimulated by insulin during wound healing. BMC Cell Biol 2009;10:1-15.
38. Lima MH, Caricilli AM, de Abreu LL, Araújo EP, Pelegrinelli FF, Thirone AC, *et al*. Topical insulin accelerates wound healing in diabetes by enhancing the AKT and ERK pathways: A double-blind placebo-controlled clinical trial. PLoS One 2012;7:e36974.
39. Chen X, Liu Y, Zhang X. Topical insulin application improves healing by regulating the wound inflammatory response. Wound Repair Regen 2012;20:425-34.
40. Nadworny PL, Landry BK, Wang J, Tredget EE, Burrell RE. Does nanocrystalline silver have a transferable effect? Wound Repair Regen 2010;18:254-65.
41. Manconi M, Manca ML, Caddeo C, Valenti D, Cencetti C, Diez-Sales O, *et al*. Nanodesign of new self-assembling core-shell gellan-transfersomes loading baicalin and in vivo evaluation of repair response in skin. Nanomedicine 2018;14:569-79.
42. Dummer W, Bastian BC, Ernst N, Schänzle C, Schwaaf A, Bröcker EB. Interleukin-10 production in malignant melanoma: Preferential detection of IL-10-secreting tumor cells in metastatic lesions. Int J Cancer 1996;66:607-10.
43. Khezri K, Farahpour MR, Mounesi Rad S. Accelerated infected wound healing by topical application of encapsulated rosemary essential oil into nanostructured lipid carriers. Artif Cells Nanomed Biotechnol 2019;47:980-8.